Journal of
Ship&Ocean
Technology
©DECEMBER 2003

SOTECH Vol. 7, No. 4, pp. 1~15, 2003

Modeling of the Formation of Long Grooves in the Seabed by Grounded Ice Keels

Aleksey Marchenko[1]

[1]Theoretical Department, General Physics Institute of RAS, Vavilova str.38, 119991 Moscow, Russia (Seoul National University, Seoul); E-mail: amarch@snu.ac.kr

Abstract

The motion of passively floating body, whose keel can have a contact with seabed soil, is under the consideration. The body simulates ice ridge floating in shallow water. The force of seabed soil reaction applied to the grounded keel is estimated taking into account soil embankment near the grounded keel. Two-dimensional trajectories of body motion, the shape of the grooves in seabed and the height of soil embankment are calculated when the motion of the body is caused by semidiurnal M_2 tide. The influence of wave amplitude and bottom slope on the shapes of body trajectory and the grooves are analyzed.

Keywords: ice ridges, ice scouring, grooves, shallow water, tides

1 Introduction

The interaction of ice keels with the underlying seabed is an important factor for the cables and pipeline systems laid upon the seabed. Grounded ice keels can cause the damage of the cables and pipelines, which not only need to be buried below the groove bottom, but also deep enough below the scour to avoid bending strains caused by soil deformations. Thus the maximal scour depth and space configuration of the grooves are most important factors influencing the design of the moored pipeline systems.

The field studies of ice scouring are carried out on the eastern Canada shelf, where the grooves are formed by drifting icebergs (Chari and Allen 1974), in the Canadian and Alaskan Beaufort sea (Clark et al 1998), on Sakhalin shelf (Astafiev et al 1997), on the shelf of Pechora sea and in Baydaratskaya Bay of Kara sea (Ryabinin et al 1995). In Sakhalin area and at Kara sea shelf the grooves are formed by grounded keels of sea ice ridges mostly at a depth 15 – 20 m in sandy or clay-sandy soils, and representative depth of the scouring is varied from 1 to 2 meters. The depth of deepest grooves reaches 4 - 5 meters at the shelf of Canadian and Alaskan Beaufort sea (Clark et al 1990). The grooves on the sea floor may extend for many kilometers.

The deepest drafts of floating sea ice ridges reach several tens meters, therefore they can impact into the seabed in shelf areas of the Arctic seas, where sea depth is of the same order. It is known that grounded ridges take a role of anchoring points for land fast ice and cause the stability of the fast ice (Wadhams 1980). Typically sea word boundary of the fast ice is related to 20 m depth, where the ridges become grounded. In the warm time of a year the level ice melt more rapid than ridges. The increasing of the amplitude of tidal wave in the absence of continuous ice causes the

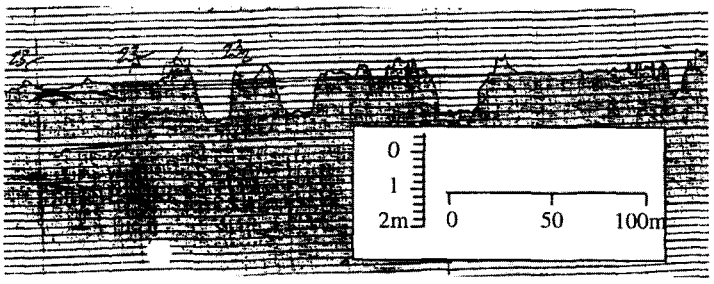

Figure 1: Example of scouring grooves by echo-sounder in Baydaratskaya Bay, Kara sea

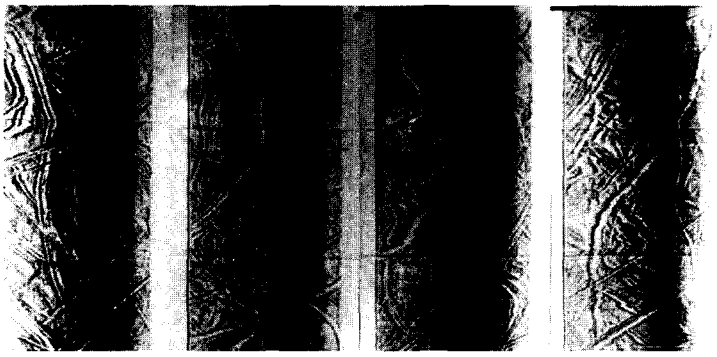

Figure 2: Fragment of side sonar data in Baydaratskaya Bay, Kara sea

floating-up of grounded ridges and their tide induced drift. We assume that the keels of passively floating ridges can impact into the seabed and create long grooves in the seabed.

Numerous field data are obtained by the using of the echo-sound profiling and side-scan sonar records (Woodworth-Lynas et al 1998, Beloshapkov and Marchenko 1998). The example of echo-sound profiling in Baydaratskaya Bay on Figure 1 shows the grooves of 1 m depth with width varied from 10 to 30 meters. The example of side-scan records on Figure 2 for the same geographical region demonstrates long curved grooves with length up to several kilometers. Representative width of floating ridge is about 50 meters (Timco and Burden 1997), while the length of ridge extension can reach several kilometers and more (Romanov 1993). The horizontal sizes of stamukhas (grounded hill-ridges) in different space directions are more homogeneous and have the order of 100 meters.

The main goal of the paper is to study the length and space configuration of scour grooves, when passively floating body imitating ice ridge interacts with bottom soil by grounded keel, whose sizes are much smaller the horizontal sizes of the body. The paper is organized as follows. In the second paragraph basic equations describing the motion of the body under the influence of water current are formulated taking into account Coriolis's effect and the elevation of water surface. In the third paragraph the formulas for semidiurnal tidal currents and seabed soil resistance are formulated. In the forth paragraph the results of numerical simulations are described. In the conclusions main results of the studies are formulated and discussed. The analytical estimations of the force of seabed soil reaction on grounded keel and equation describing the changes of embankment height near grounded keel are formulated in the Appendix.

2 Basic equations

Equation of momentum balance of passively floating body in the projection on horizontal plane is formulated as follows

$$M\left(\frac{d\mathbf{v}}{dt}+\mathbf{f}\times\mathbf{v}\right)=\mathbf{F}_w+\mathbf{F}_{soil} \tag{1}$$

where M is the mass of the body, $\mathbf{v}=(v_x,v_y)$ is the vector of body velocity, $\mathbf{f}\times\mathbf{v}=f(-v_y,v_x)$ denotes Coriolis's force with $f=2\Omega\sin\Phi$, $\Omega\approx 0.7\cdot 10^{-5}s^{-1}$ is the frequency of Earth rotation and Φ is the latitude angle, $\mathbf{F}_w$ and $\mathbf{F}_{soil}$ are the horizontal components of forces applied to body surface by water and seabed soil.

We write force $\mathbf{F}_w$ as the sum of horizontal projections of resulting hydrostatic pressure $\mathbf{F}_{hst}$ applied to body surface and dynamic pressure $\mathbf{F}_{dyn}$ due to body motion relatively water

$$\mathbf{F}_w=\mathbf{F}_{hst}-F_{hst,z}\mathbf{e}_z+\mathbf{F}_{dyn} \tag{2}$$

where $F_{hst,z}$ is vertical component of the force $\mathbf{F}_{hst}$, and $\mathbf{e}_z$ is vertically directed unity vector. The force $\mathbf{F}_{hst}$ is written as follows

$$\mathbf{F}_{hst}=-\int\limits_{S_w}p_{hst}\mathbf{n}ds,\quad p_{hst}=\rho_w g(\eta-z) \tag{3}$$

where p_{hst} is hydrostatic water pressure, function $\eta(t,x,y)$ describes the elevation of water surface, z is vertical coordinate, $\mathbf{n}$ is outward normal to submerged body surface, and ρ_w is water density.

Perturbations introduced in the water by body motion are small when body sizes are much smaller of horizontal scale of water motions and water velocity is compared with body velocity. In that case we can extend function $\eta(t,x,y)$ into the region of body location and set that equation $z=\eta(t,x,y)$ describes water surface elevation in the absence of the body. The integral in formula (3) can be written as $\mathbf{F}_{hst}=-\int_{\partial S_w}p_{hst}\mathbf{n}ds$, where the surface ∂S_w consists of wetted body surface and the surface described by equation $z=\eta(t,x,y)$. Applying the Stokes theorem to the last integral one finds

$$\mathbf{F}_{hst}=\rho_w g V_w(-\nabla\eta+\mathbf{e}_z) \tag{4}$$

where $\nabla\eta=\mathbf{e}_x\partial\eta/\partial x+\mathbf{e}_y\partial\eta/\partial y$, $\mathbf{e}_x$, $\mathbf{e}_y$ are horizontally directed orthogonal unity vectors, and V_w is the volume of submerged part of the body.

It is assumed that the body is floating in almost hydrostatic equilibrium, and only small part of body keel, called as grounded keel, can penetrate into the seabed (Figure 1). In that case the mass of the body is equal to $M=\rho_w V_w$, and horizontal projection of resulting hydrostatic pressure is equal to

$$\mathbf{F}_{hst}-F_{hst,z}\mathbf{e}_z=-Mg\nabla\eta \tag{5}$$

The dynamic force is estimated as follows

$$\mathbf{F}_{dyn}=M_{ad}\frac{d(\mathbf{v}_w-\mathbf{v})}{dt}+\rho_w C_w S_{ef}|\mathbf{v}_w-\mathbf{v}|(\mathbf{v}_w-\mathbf{v}) \tag{6}$$

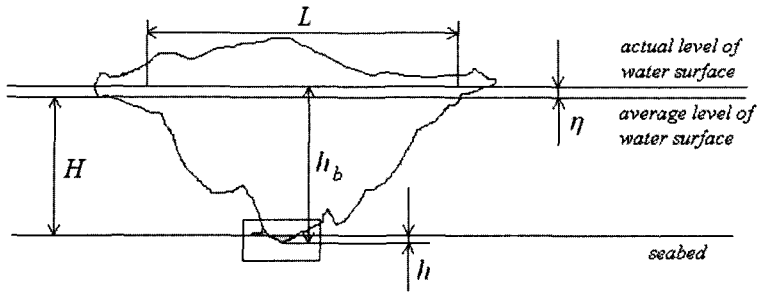

Figure 3: Floating ice ridge with grounded keel. The scheme of the motion of seabed soil in the vicinity the square is shown at Figure 9

where $\mathbf{v}_w = (v_{w,x}, v_{w,y})$ is horizontal velocities of the water around the body, M_{ad} is the added mass of the body, C_w is drag coefficient and S_{ef} is representative area of the vertical cross-section of the body.

The force of seabed soil reaction is written in the following form

$$\mathbf{F}_{soil} = -hwK\frac{\mathbf{v}}{|\mathbf{v}|}, \quad |\mathbf{v}| > 0, \quad h > 0 \tag{7}$$

where h is the depth of the penetration of grounded keel into the seabed (Figure 3), and w is the width of the keel (Figure 9). The product hw is representative area of contact surface of grounded keel with unperturbed seabed. Coefficient K depends on the configuration of body keel - seabed soil contact surface, soil cohesion and other parameters, characterizing the interaction of body keel with seabed soil. In the Appendix the upper and lower bounds of the coefficient K are found using the maximum-dissipation principle. When $\mathbf{v} = 0$ the force $\mathbf{F}_{soil}$ is defined from (1). The body starts to move when condition $|\mathbf{F}_{soil}| = hwK$ becomes satisfied. The depth of the penetration of grounded keel into the seabed is defined by formula

$$h = h_b - (\eta + H) \tag{8}$$

where h_b is the draft of the body, and H is the depth of unperturbed water (Figure 3).

We set $\mathbf{F}_{soil} = 0$ when $h < 0$. In that case equation (1) with formulas (2), (4) and (5) is written as follows

$$\frac{d\mathbf{v}}{dt} + \mathbf{f} \times \mathbf{v} = -g\nabla\eta + \mathbf{F}_{dyn}/M \tag{9}$$

Assuming that water motion is described by linearized shallow water equations

$$\frac{\partial \mathbf{v}_w}{\partial t} + \mathbf{f} \times \mathbf{v}_w = -g\nabla\eta, \qquad \frac{\partial \eta}{\partial t} + \nabla \cdot (H\mathbf{v}_w) = 0 \tag{10}$$

and taking into account that $\mathbf{F}_{dyn} = 0$ when $\mathbf{v} = \mathbf{v}_w$, we find that equation (9) has solution $\mathbf{v} = \mathbf{v}_w$, describing body motion together with surrounding water. The influence of the force $\mathbf{F}_{soil}$ changes the body motion. The friction between water and bottom is not considered since it is much smaller the force $\mathbf{F}_{soil}$.

3 Ice bottom scouring under the influence of semi-diurnal tide

Explicit solution of (10) called as Sverdrup wave is described by formulas (Kowalik and Marchenko 2002)

$$\eta = a\cos(kx+\omega t), \quad v_{w,x} = \frac{ag\omega k}{f^2-\omega^2}\cos(kx+\omega t), \quad v_{w,y} = -\frac{agfk}{f^2-\omega^2}\sin(kx+\omega t) \quad (11)$$

where a, ω and k are wave amplitude, wave frequency and wave number. Further it is assumed that wave frequency $\omega = 1.4\cdot 10^{-4}s^{-1}$ is related to the period 12.42 hours of M_2 semi-diurnal tide, and $f = 1.36\cdot 10^{-4}s^{-1}$ is related to the value of Coriolis's parameter at the latitude angle $\Phi = 70°$. Wave frequency ω is related to wave number k by the dispersion equation

$$\omega^2 - f^2 = gHk^2 \quad (12)$$

where H is water depth. It is assumed that water depth is changed slowly near the value $H_0 = 20m$. Therefore for the calculation of wave number k we set in (12) $H = H_0$.

The draft of the body is equal to h_b, and horizontal size of the body is characterized by length L (Figure 3). Since the body is floating almost in hydrostatic equilibrium the mass of the body is estimated as $M = \rho_w h_b L^2$, and representative area of the vertical cross-section of the body is estimated as $S_{ef} = h_b L$. It is assumed that added mass of the body is equal to $M/2$ as for submerged sphere. For the numerical estimations we set $h_b = 20m$, $L = 100m$ and $w = 10m$.

The motion of the body is described by equation of momentum balance (1), the dynamic force is defined by formulas (6), and the projection of the force of seabed reaction on horizontal plane is defined by formula (7). Coefficient K in formula (7) is defined according to formula (A15) as follows

$$K = k_1\tau + k_2 h_{em}, \quad k_1 = 2(1+\theta), \quad 2k_2 = \gamma(\rho_s - \rho_w)g \quad (13)$$

where τ and ρ_s are the cohesion and density of seabed soil, h_{em} is the height of the embankment from seabed soil around the grounded keel, θ is slope angle of the grounded keel (Figure 9), parameter γ characterizes the porosity of seabed soil in the embankment. Formulas (7) and (13) define lower bound of the horizontal projection of seabed resistance. We use the lower bound for the finding of upper bound of the depth and the length of grooves formed in seabed by grounded keels.

In numerical simulations the following representative values are used

$$\tau = 10 \text{ kPa}, \quad \rho_s = 2000 \text{ kg}\cdot m^{-3}, \quad \rho_w = 1000 \text{ kg}\cdot m^{-3}, \quad \theta = 30°, \quad \gamma = 0.8 \quad (14)$$

The variation of the height of embankment soil h_{em} is defined by (A16), where the angle of the embankment slope is $\varphi = 30°$. Drag coefficient $C_w = 1$ characterizing the dynamic force is chosen as for purely streamlined bodies (Robe 1980).

The penetration of grounded keel into the seabed is defined by formula (8), where the depth $H = H_0 + \delta H(x,y)$ with $\delta H << H_0$ is given as a function of the location of the body. The location of the body is defined by equations

$$\frac{dx}{dt} = v_x, \quad \frac{dy}{dt} = v_y \quad (15)$$

Formulas (11) and (15) define the elevation of water surface depending on body location.

4 Results of numerical simulations

The system of equations describing the variations of functions $x(t)$, $y(t)$, $v_x(t)$, $v_y(t)$ and $h_{em}(t)$ consists of equations (1), (15) and (A16). Forcing terms in these equations are defined by formulas (6) and (13). Initial conditions are $x(0) = y(0) = 0$, $v_x(0) = v_y(0) = 0$ and $h_{em}(0) = 0$. Further the results of numerical simulations are described.

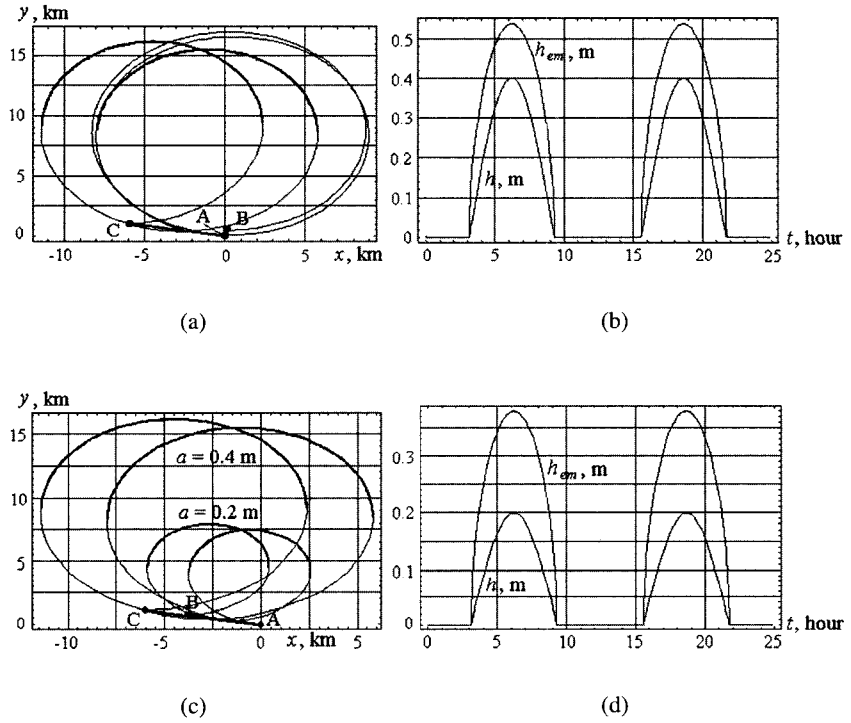

Figure 4: Trajectories of the floating body (curve AC) and water particles (thin curve AB) moving by semidiurnal tide with amplitude $a = 0.4$m in the water of constant depth $H = 20$m (a); trajectories of the floating body moving by semidiurnal tide with amplitude $a = 0.4$ m(curve AC) and $a = 0.2$ m(curve AB) in the water of constant depth $H = 20$m (c); the dependencies of grooves depth h and the height of the embankments h_{em} from the time for $a = 0.4$ m (b) and $a = 0.2$ m (d). Thick segments of the curves on Figures (a) and (c) show the grooves in the seabed

Figure 4a shows trajectory AB of water particles moving by semidiurnal tide with amplitude 0.4 m during two M_2 wave periods (~25 hours) in the water of constant depth $H = 20$ m. The beginning of the trajectory (point A) is almost coincides with the end of the trajectory (point B) because a small wave drift. The curve AC shows the trajectory of the motion of passively floating body whose keel penetrates into the seabed at two arched segments of the trajectory denoted by thick lines. The length of each groove is more then 15 km. Straight line segment AC with length about 6 km shows the resulting drift of the body during two wave periods in the direction of wave propagation. The drift is deviated to the right from the direction of wave propagation due to the Coriolis's effect. Figure 4b shows the dependence of grooves depth h and the height of soil

embankment h_{em} from the time t. One can see that maximal depth of the grooves is equal to wave amplitude 0.4 m, and maximal height of the embankment is about 0.54 m.

Figure 4c shows the influence of tidal wave amplitude on the grooves in the case of constant water depth $H = 20$ m. The values of wave amplitudes are shown at Figure 4c. The decreasing of wave amplitude causes the decreasing of grooves lengths and the decreasing of the resulting drift characterized by straight linear intervals AB for amplitude 0.2 m and AC for amplitude 0.4 m. Figure 4d shows groove depth h and the height of soil embankment h_{em} versus the time t when wave amplitude is equal 0.2 m. Figures 4b and 4d show that groove depth and the height of soil embankment becomes smaller with the decreasing of wave amplitude. [hb]

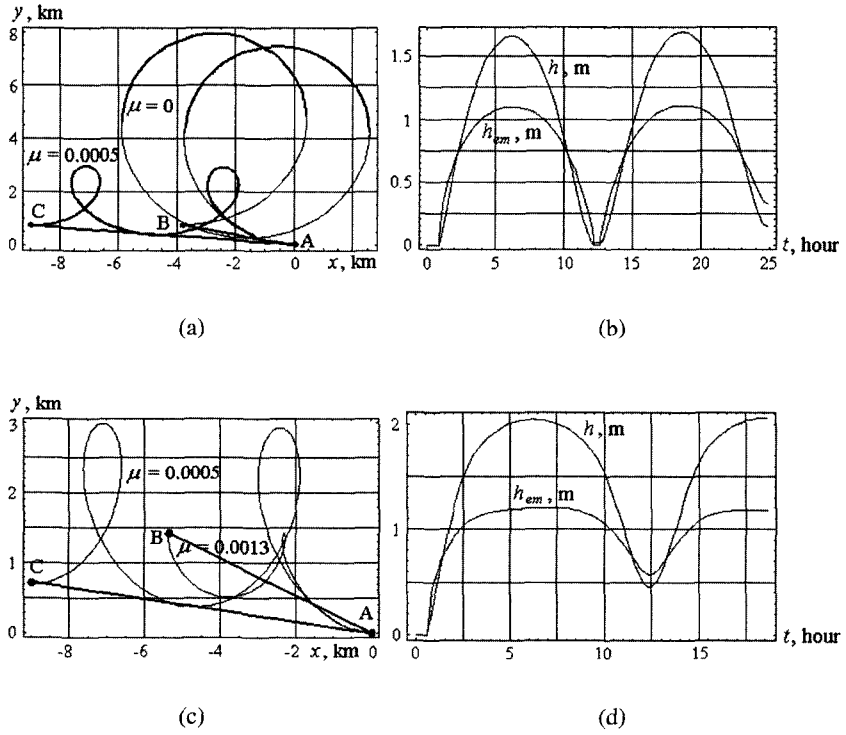

Figure 5: Trajectories of the floating body moving by semidiurnal tide with amplitude $a = 0.2$ m in the water of variable depth $H = H_0 - \mu y\theta(y)$, where $\theta(y)$ is unit step function (a, c); the gouge depth h and the height of soil embankment h_{em} versus the time for $\mu = 0.0005$ (b) and $\mu = 0.0013$ (d). The values of μ are shown at the figures. Thick segments of the curves on Figure (a) show the grooves in the seabed

Figures 5 show the influence of sea bottom slope in the y-direction on the shape of the grooves. It is assumed that the shape of sea bottom is defined by formula $H = H_0 - \mu y\theta(y)$, where $H_0 = 20$ m and $\theta(y)$ is unit step function equaling 1 when $y > 0$ and 0 when $y < 0$. The values of parameter μ are shown at Figures 5a and 5c. Small increasing of bottom slope from $\mu = 0$ to $\mu = 0.0005$ causes the increasing of body drift during two wave periods and the decreasing of drift deviation to the right relatively the direction of wave propagation. Body drift reaches 9 km per 25 hours when $\mu = 0.0005$ due to the decreasing of the length of segments, where the body

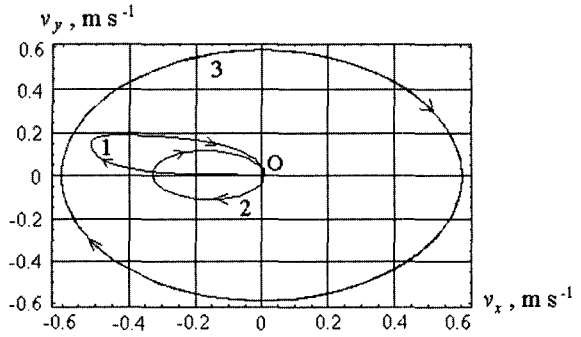

Figure 6: Hodograph of the velocity of the floating body moving by semidiurnal tide with amplitude $a = 0.2$m in the water with variable depth with $\mu = 0.0013$ (loops 1 and 2); hodograph of the velocity of water particles (loop 3) moving by the same tide

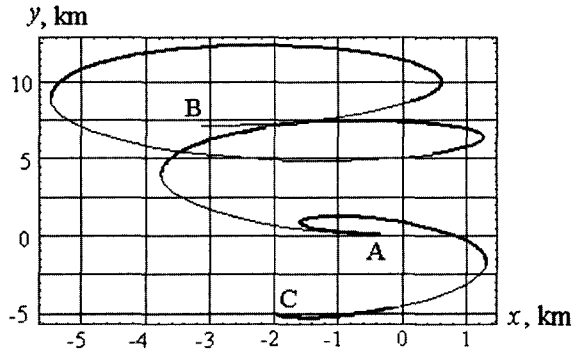

Figure 7: Trajectories of the floating body moving by semidiurnal tide with amplitude $a = 0.2$m in the water of variable depth $H = H_0 - \mu x\theta(x)$ (curve AB) and $H = H_0 + \mu x\theta(-x)$ (curve AC) with $\mu = 0.001$

moves in the opposite direction to wave propagation. In the case $\mu = 0.0005$ the groove coincides with the body trajectory and has folded shape (thick curve AC on Figure 5a and thin curve AC on Figure 5c). The floating body is stopped during 19 hours when $\mu = 0.0013$ (Figure 5c), and the groove AB consists of two arched segments.

The decreasing of water depth in the y-direction causes more early penetration of the keel into the seabed in comparison with the case of constant water depth. From Figure 4b it follows that the first contact of the keel with seabed soil is occurred 3 hours later the beginning of the motion in the case of constant depth. Figure 5b and 5d shows that the time of the first contact is shortened up to 1 hour when $\mu = 0.0005$ and $\mu = 0.0013$. In these cases the groove is formed during almost all time of body motion, and maximal height of the embankments are smaller maximal values of groove depths. Maximal depth of the groove is equal to 2m and maximal height of the embankment is about 1.25 m when $\mu = 0.0013$ (Figure 5d).

Figure 6 demonstrates the hodograph of the velocity of the floating body moving by semidiurnal tide with amplitude 0.2 m when bottom slope in the y-direction is characterized by $\mu = 0.0013$ and the hodograph of water particles moving by the same tide. The hodograph of body velocity consists of two loops denoted as 1 and 2. The first loop is related to body motion during first 5

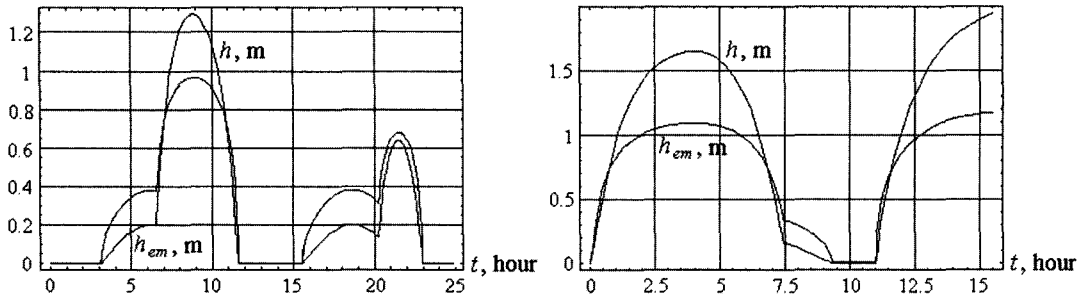

(a) (b)

Figure 8: The dependencies of groove depth h and embankment height h_{em} from the time when $H = H_0 - \mu x\theta(x)$ (a) and $H = H_0 + \mu x\theta(-x)$ (b) with $\mu = 0.001$

hours. The variations of groove depth and embankment height are shown at Figure 5d for that case. One can see the groove depth and the embankment height are almost constants when the time is changed from 5 hours to 7.5 hours. In this time body velocity is very small and the end of the vector of body velocity is around the origin at Figure 6. Then the end of the vector of body velocity is following by loop 2 until the origin. Loop 3 is related to the periodic motion of water particles.

Figures 7 and 8 demonstrate the influence of variable depth in the x-direction on body motion. Curve AB at Figure 7 and Figure 8a show respectively the trajectory of the body and the variations of grooves depth and embankment height when water depth is increased in the opposite direction to wave propagation: $H = H_0 - \mu x\theta(x)$ with $\mu = 0.001$. The grounded keel creates two arched grooves during two wave periods lied on the curve AB. Curve AC at Figure 7 and Figure 8b show the same quantities for the case when water depth increases in the direction of wave propagation: $H = H_0 + \mu x\theta(-x)$ with $\mu = 0.001$. From Figure 7 one can see that in the first case the body drifts away the bottom slope by tide, and therefore grooves depth become smaller with the time (Figure 8a). In the second case the body moves during $\sim$15 hours and then stops. The grooves have maximal depth about 2 m in the end of the motion (Figure 8b). In the both cases grooves depth are greater than the height of the embankment during almost all time of the motion.

5 Conclusions

The model describing the motion of passively floating body whose keel has a contact with the seabed is elaborated. It is assumed that only a small part of the body called as grounded keel has a contact with seabed soil. The force of seabed soil reaction applied to the grounded keel is estimated using the maximum-dissipation principle for large deformations of seabed soil. The model gives possibility to calculate the trajectory of body motion in the horizontal plane, the shape of the grooves formed by grounded keel and the height of soil embankment near the grounded keel. The elaborated model describes the formation of long grooves in the seabed by the keels of floating sea ice ridges in shallow water areas of seas covered by the ice in the cold time of a year.

Numerical simulations were carried out for the case when body motion is caused by Sverdrup

wave with the frequency of semidiurnal M_2 tide. It is assumed that water depth and body draft are about 20 m, horizontal sizes of the body have the order 100 m, and seabed soil cohesion is 10 kPa. The influence of wave amplitude and bottom topography on body motion, grooves shape and the height of soil embankments was studied. The main results are as follows:

- Periodical contact of body keel with seabed creates the drift of the body in the direction of wave propagation. The drift is more strong that wave drift of water particles. Calculated body drift in the water of constant depth 20 m is about 7 km per 25 hours (doubled wave period) when wave amplitude is 0.4 m.
- The drift has deviation to the right in the Northern hemisphere due to the Coriolis's effect.
- The embankment height is bigger grooves depth, and maximal grooves depth are equal to the amplitude of tidal wave when the water depth is constant.
- Slow decreasing of water depth in perpendicular direction to wave propagation causes the increasing of body drift during two wave periods after the beginning of the motion. Calculated body drift in the water with bottom slope 0.0005 is about 9 km per 25 hours when wave amplitude is 0.2 m.
- The increasing of bottom slope up to 0.0013 creates the stop of the body 19 hours later the beginning of the motion.
- Maximal embankment height is smaller maximal grooves depth in the case of bottom slope. Calculated maximal value of grooves depth is about 2 m.
- The bottom slope in the direction of wave propagation causes the stop of the body more quickly then in the case when bottom slope is perpendicular to wave propagation.
- Maximal calculated length of the grooves is about 15 km. Most typical shape of the grooves is arched. In the case of small bottom slope the folded shapes of grooves are possible also.

Acknowledgement

I would like to thank Prof. Hyochul Kim for the support of this work in the Seoul National University, and to Prof. Andrey Kulikovskii for useful comments. The work is supported by Russian Foundation for Basic Research (02-01-00729).

References

ASTAFIEV, V.N., SURKOV, V.N. AND TRUSKOV, P.A. 1997 Hummocks and stamukhas in Okhotsk sea. St.-Petersburg, Progress-Pogoda, in Russian, pp. 184

BELOSHAPKOV, A., MARCHENKO, A., DLUGACH, A. 1998 Seabed exaration by ice formations. Proc. Ice Scour and Arctic Marine Pipeline Workshop. 13the Int Symp on Okhotsk Sea and Sea Ice., Mombetsu, Hokkaido, Japan, February 1-4, 1998, pp. 101-120

BELOSHAPKOV, A. AND MARCHENKO, A. 1998 Mathematical modeling of ice bottom scouring in Baydaratskaya Bay. Ice in Surface Waters, Shen (ed), 1998 Balkema, Rotterdam, ISBN 9054109718, pp. 345-352

CHARI, T.R. AND ALLEN, J.N. 1974 An analytical model and laboratory tests on iceberg sediment interaction. Proc. IEEE Int. Conf. Eng. in the Ocean Environment. New-York: Inst. of Electrical and Electronic Engineers, Inc. 1: pp. 133-136

CHOI, K., LEE J. 2003 A comparative study of ice ridge - seabed interaction models. Proc. Int. Workshop on Frontier Technology in Ship and Ocean Eng., pp. 159-170

CLARK, J.L., PAULIN, M.J. AND POOROOSHASB, F. 1990 Pipeline stability in an ice-scoured seabed. Proc. First European Offshore Mechanics Symp., Trondheim, Norwey, pp. 533-549

CLARK, J.L., PHILLIPS, R. AND PAULIN, M.J. 1998 Ice scour research for the safe design of pipelines: 1978-1998. Proc. Ice Scour and Arctic Marine Pipeline Workshop. 13the Int Symp on Okhotsk Sea and Sea Ice, Mombetsu, Hokkaido, Japan, February 1-4, 1998, pp. 1-7

FORIERO, A. 1998 Steady-state ice scouring of the seabed. Proc. Ice Scour and Arctic Marine Pipeline Workshop. 13the Int Symp on Okhotsk Sea and Sea Ice., Mombetsu, Hokkaido, Japan, February 1-4, 1998, pp. 83-99

KOWALIK, Z. AND MARCHENKO, A. 2002 Tidal motion enhancement around islands. J. Marine Research, **60(4)**, pp. 551-581

ROBE, R.Q. 1980 Iceberg drift and deterioration. Dynamics of Snow ans Ice Masses, S. Colbeck (ed), Academic Press, New-York, pp. 211-259

ROMANOV, I.P. 1993 Atlas; Morphometric Characteristics of Ice and Snow in the Arctic Basin. St.-Petersburg: Arctic and Antarctic Research Institute

RYABININ, V.E., DANILOV, A.I., ELISOV, V.V., KLEPIKOV, A.V., KURDUMOV, V.A., MALEK, V.N., SMIRNOV, V.N., STEPANOV, I.V. AND TIMOFEEV, O. YA. 1995 Marine ice bottom gouging: some mechanisms and an approach to depth evaluation. Proc. Sea Ice Mech. and Arctic Modeling Workshop, Anchorage, Alaska, **2**, pp. 276-285

TIMCO. G. M. AND BURDEN, R.P. 1997 An analysis of the shapes of sea ice ridges. Cold Reg. Sci. Techn., **25**, pp. 65-77

WADHAMS, P. 1980 Ice characteristics in the seasonal sea ice zones. Cold Reg. Sci. Techn., **2**, pp. 37-87

WOODWORTH, C.M.T., PHILLIPS, R., CLARK, J.I., HYNES, F. AND XIAO, X. 1998 Verification of centrifuge model results against field data: results from the pressure ridge ice scour experiment (PRISE). Proc. Ice Scour and Arctic Marine Pipeline Workshop. 13the Int Symp on Okhotsk Sea and Sea Ice, Mombetsu, Hokkaido, Japan, February 1-4, 1998, pp. 123-138

Appendix

Upper and lower bounds of seabed resistance

There are different approaches for the calculation of the reaction of seabed soil. The first most simple and practically defensible method is based on the using of two-dimensional Prandtl solution of ideal plasticity describing the penetration of the stamp in a half-space (Chari and Allen 1974). Later this method was modified to take into account pressure dependent plastic condition, which is more adapted for soil mechanics (Ryabinin et al 1995, Choi and Lee 2003). Foriero (1998) formulated the method of the calculation of the seabed reaction based on the consideration of a creeping deformation of soil. Beloshapkov and Marchenko (1998) developed the method of the estimation of the upper and lower bounds of the seabed reaction in three-dimensional problems using the maximum-dissipation principle for large deformation of seabed soil. Further we extend

this method taking into account the influence of soil embankment in the front of grounded keel.

It is assumed that internal stresses σ_{ij} in the bottom soil satisfy to static equilibrium equations

$$\sum_{j=x,y,z} \frac{\partial \sigma_{ij}}{\partial x_j} = 0 \tag{A1}$$

where i and j are running over the values x, y, z. It is assumed that gravity force is much smaller internal stresses necessary to press out the soil on seabed surface by grounded keel. Therefore the gravity force is omitted in (A1).

The maximum-dissipation principle for plastic deformations of bottom soil is formulated as follows

$$(\sigma_{ij} - \sigma^*_{ij}) e_{ij} \geq 0 \tag{A2}$$

where σ_{ij} and e_{ij} are stresses and strain rates for a process of plastic deformation and σ^*_{ij} are arbitrary admissible stresses located inside the yield surface. It is assumed that yield surface is defined by the Tresca condition, and plastic shear is occurred when maximal shearing stress takes the critical value $2\sqrt{2}\tau$.

Let us consider the soil motion near the front of the grounded keel impacted into the seabed. The region under the consideration is shown on Figure 9. The soil fills half-plane $z < 0$ with the exception of the groove made by the keel. It is assumed that normal and shearing stresses are equal to zero on seabed surface with exception of the region below the embankment, where normal stress is equal to the weight of embankment column. Normal velocity of soil particles is equal to body velocity $\mathbf{v}$ on the frontal face of grounded keel.

Let us assume that σ_{ij} and e_{ij} are some stresses and strain rates coupled by associated flow rule and satisfying the boundary conditions, and σ^*_{ij} are actual stresses. Integrating (A2) over the volume occupied by seabed soil and using the Stokes theorem we find

$$\int_V \sigma_{ij} e_{ij} dV \geq \int_S \sigma^*_{ij} v_i n_j dS \tag{A3}$$

where V is the volume occupied by seabed soil, S is the surface of bottom soil and n_j are the components of outward normal vector to the surface S.

For the finding of tensors σ_{ij} and e_{ij} we consider the scheme of the motion of seabed soil, when the soil prism P_1 (Figure 9) is pressed out from the seabed by grounded keel. From the equality of normal projections of the velocity $\mathbf{v}_s$ of soil prism P_1 and ice ridge velocity $\mathbf{v}$ on the forward face of grounded keel it follows

$$\mathbf{v} = (-v, 0, 0), \quad \mathbf{v}_s = -v\frac{\cos\theta}{\sin\psi}(\sin(\psi+\theta), 0, -\cos(\psi+\theta)) \tag{A4}$$

where angles ψ and θ are shown at Figure 9.

In coordinates $(\xi, \varsigma, \lambda)$ the components of plastic strain rate tensor are defined as follows

$$e_{\xi\xi} = e_{\varsigma\varsigma} = e_{\lambda\lambda} = e_{\varsigma\lambda} = 0, \quad 2e_{\xi\varsigma} = v_s(\delta(\varsigma - w) - \delta(\varsigma)), \quad 2e_{\xi\lambda} = v_s\delta(\lambda) \tag{A5}$$

where $v_s = |\mathbf{v}_s|$, δ denotes Dirac delta function and w is the width of grounded ice keel. Stress tensor satisfying the Tresca condition and associated flow rule is defined by formulas

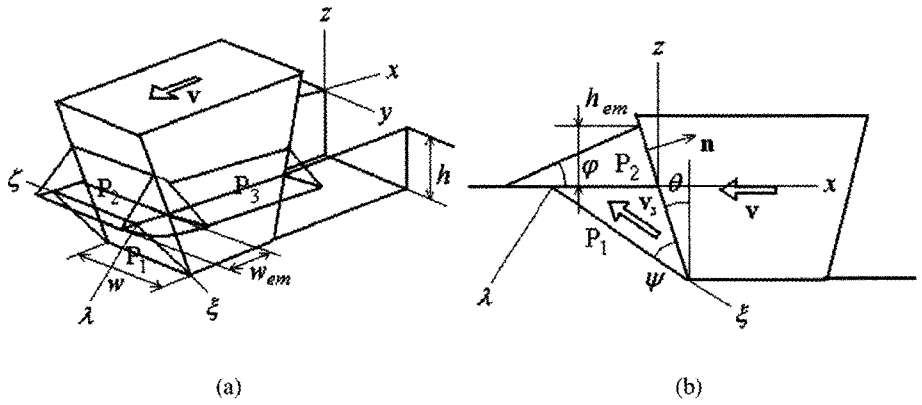

Figure 9: The scheme of the motion of bottom soil in the vicinity of grounded ice keel. P_1 is soil prism pressed out by the grounded keel from unperturbed seabed with velocity $\mathbf{v}_s$, P_2 is soil embankment moving in the front of the keel, P_3 is soil embankment superincumbent on the surface of unperturbed seabed

$$\sigma_{\xi\xi} = \sigma_{\varsigma\varsigma} = \sigma_{\lambda\lambda} = \sigma, \quad \sigma_{\varsigma\lambda} = 0, \quad \sigma_{\xi\lambda} = \tau, \quad \sigma_{\xi\varsigma} = \pm\tau \tag{A6}$$

where signs "+" and "-" are related to lateral surfaces of prism P_1 by $\varsigma = w$ and $\varsigma = 0$ respectively. From formulas (A5) and (A6) it follows

$$\int_V \sigma_{ij} e_{ij} dV = \tau h w v K_1 \cos\theta, \quad K_1 \sin\psi = \frac{1}{\cos(\psi+\theta)} + \frac{h}{w}(\tan(\psi+\theta) - \tan\theta) \tag{A7}$$

Assuming that shearing stresses are much smaller normal stresses at the face of grounded keel we write the stress σ_n applied to this face by the keel as follows

$$\sigma_n = -\sigma_n \mathbf{n} \tag{A8}$$

where unity normal $\mathbf{n}$ at the face in (x, y, z) coordinates is defined as $\mathbf{n} = (\cos\theta, 0, \sin\theta)$ (Figure 9b). Using formulas (A4) and (A8) the integral in the right part of inequality (A3) is calculated as

$$\int_S \sigma^*_{ij} v_i n_j dS = -R_n \mathbf{n} \cdot \mathbf{v}_s - p_{em} S_1 \mathbf{v}_s \cdot \mathbf{e}_z \tag{A9}$$

where R_n is the absolute value of normal force at the face of grounded keel, p_{em} is averaged pressure of the embankment on the seabed in the front of grounded keel, quantity $S_1 = wh(\tan(\varphi + \theta) - \tan\theta)$ is equal to the area of top surface of prism P_1, and $\mathbf{e}_z = (0, 0, 1)$ is vertically directed unity vector.

Assuming that the embankment in the front of grounded keel has the shape of prism P_2 we express the volume of the prism as

$$V_{P2} = w\frac{h_{em} w_{em}}{2}, \quad w_{em} = h_{em}\left(\frac{1}{\tan\varphi} + \tan\theta\right) \tag{A10}$$

where w_{em} is the length of the embankment in the x-direction shown on Figure 9a.

The weight of the embankment is distributed over the area ww_{em}. Taking into account buoyancy force the pressure p_{em} is estimated as

$$p_{em} \approx \frac{\gamma(\rho_s - \rho_w)}{2} g h_{em} \tag{A11}$$

where ρ_s is the density of seabed soil and γ is soil concentration in the embankment. Parameter γ characterizes friability of the soil composing the embankment.

Taking into account formulas (A4), (A7), (A9) and (A11) inequality (A3) is formulated as

$$K_1 + K_2 \geq \frac{R_n}{wh\tau}, \quad K_2 = (\tan(\varphi + \theta) - \tan\theta)\frac{\cos(\psi + \theta)}{\cos\psi}\frac{p_{em}}{\tau} \tag{A12}$$

The upper bound (A12) can be improved by minimizing of sum $K_1 + K_2$ with respect to angle ψ. Quantities $\tau = 10$ kPa, $\rho_s = 2000$ kg $\cdot$ m^{-3} and $\varphi = \pi/6$ are representative values of the cohesion of sandy - clayey soils, their density and the angle of internal friction. Representative values of depth h and width w of grounded keel are 1 m and 10 m. The values of angle ψ minimizing sum $K_1 + K_2$ are equal to 0.9, 0.6 and 0.45, when $h_{em} = 3$ m and $\theta = 0$, $\pi/6$ and $\pi/4$ respectively. Using formulas (A7) and (A12) we have $K_1|_{\theta=0} \approx 2.2$, $K_2|_{\theta=0} \approx 0.5$, $K_1|_{\theta=\pi/6} \approx 5$, $K_2|_{\theta=\pi/6} \approx 1$, $K_1|_{\theta=\pi/4} \approx 10.5$, $K_2|_{\theta=\pi/4} \approx 2.4$.

Let us assume that σ_{ij} and e_{ij} are actual stresses and strain rates, and σ^*_{ij} is explicit solution of some problem about static equilibrium of the soil. Integrating (A2) over the volume occupied by seabed soil we find

$$\int_S \sigma_{ij} v_i n_j dS \geq \int_S \sigma^*_{ij} v_i n_j dS \tag{A13}$$

The solution of Prandtl problem (Figure 10) about the loading of obtuse angle by the constant

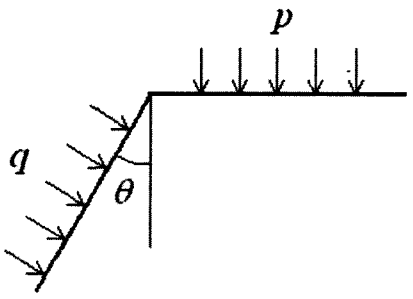

Figure 10: The loading of obtuse angle by the constant normal active load q applied to one side. The other side is under the constant normal passive load p

normal active load q applied to one side, while the other side is under the constant normal passive load p

$$q = 2\tau(1 + \theta) + p \tag{A14}$$

It is assumed that active load q is equal to normal stress $\sigma_{ij}^{*} n_i n_j$ at the face of grounded keel, and passive load $p \approx p_{em}$, where p_{em} is defined by formula (A11). Inequality (A13) with using formulas (A8), (A11) and (A14) is written as follows

$$\frac{R_n}{whr} \geq K_3, \quad K_3 = \frac{2(1+\theta)+\beta}{\cos\theta} \tag{A15}$$

Simple calculations show that $K_3|_{\theta=0} \approx 3.1$, $K_3|_{\theta=\pi/6} \approx 4.8$, $K_3|_{\theta=\pi/4} \approx 6.7$ when $h_{em} = 3$ m. One can see K_3 becomes closed to $K_1 + K_2$ when $\theta \to 0$. Estimations (A12) and (A15) give also a good accuracy ~20% when $\theta = \pi/6$.

Dynamics of soil embankment near grounded keel

The law of mass balance of seabed soil in the vicinity of the embankment is formulated as follows

$$\gamma\rho_s \frac{dV_{em}}{dt} = F_{bs} - F_{em} \tag{A16}$$

where $V_{em} = V_2 + 2V_4 + 2V_5$ and V_2, V_4 and V_5 are the volumes of prism P_2, quarter of the cone P_4 and prism P_5 (Figure 11), $F_{bs} = \rho_s vhw$ is the flux of seabed soil from the seabed, $F_{em} = \rho_s v\gamma h_{em}^2 \tan^{-1}\varphi$ is the flux of embankment soil into the lateral embankments P_3. The volume V_{em} is equal to

$$V_{em} = \frac{h_{em}^2}{2\tan\varphi}\left(w\left(1+\tan\varphi\tan\theta\right) + \frac{\pi h_{em}}{3\tan\varphi} + 2h_{em}\tan\theta\right) \tag{A17}$$

The equilibrium sizes of the embankment are defined from condition $F_{bs} = F_{em}$ as follows

$$h_{em} = \sqrt{hw\gamma^{-1}\tan\varphi} \tag{A18}$$

Assuming $h = 1$ m, $w = 10$ m, $\gamma = 0.8$ and $\varphi = \pi/6$ one finds $h_{em} \approx 2.7$ m.

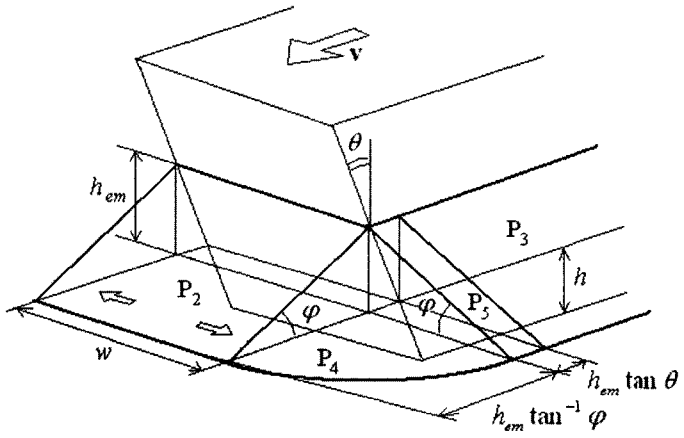

Figure 11: The scheme of soil embankment near the grounded keel